JCTC Journal of Chemical Theory and Computation

Optical Absorptions of New Blue-Light Emitting Oligoquinolines Bearing Pyrenyl and Triphenyl Endgroups Investigated with Time-Dependent Density Functional Theory

Jianmin Tao*,† and Sergei Tretiak‡

Theoretical Division and Center for Nonlinear Studies and Center for Integrated Nanotechnology, Los Alamos National Laboratory, Los Alamos, New Maxico 87545

Received December 1, 2008

Abstract: The optical absorption spectra of a family of four n-type conjugated oligomers, oligoquinolines, which can be commercially used to develop high-performance light-emitting diodes for their many desirable properties, have been recently calculated from time-depedent density functional theory (TDDFT) within the adiabatic approximation for the dynamical exchange-correlation potential. In this work, we investigate the optical absorption of two new family members of the blue-light emitting oligoquinolines bearing pyrenyl and triphenyl endgroups in gas phase and chloroform ($CHCl_3$) solution employing the adiabatic TDDFT. The ionization potentials and electron affinities of these two oligoquinoline molecules are also calculated with the ground-state DFT, from which the adiabatic dynamical exchange-correlation potential is constructed. We show that the calculated optical absorptions are in good agreement with experiments. The ionization potentials obtained with the DFT methods agree well with the experimental estimates, while the electron affinities are significantly underestimated in comparison with experiments. A natural transition orbital analysis for selected excited states with the largest oscillator strengths shows that the electronic charge is slightly redistributed in the process of electronic excitations.

I. Introduction

In recent years, n-type (electron transport) organic light-emitting materials have been increasingly gaining popularity in the development of high-performance organic light-emitting diodes (OLEDs)[1,2] because of their ultralow cost, light weight, and flexibility. A common feature of these nanoscale molecules is that they have a backbone chain with overlapping π orbitals. On the one hand, they exhibit the property of a semiconductor because the π orbitals form delocalized valence-band hole and conduction-band electron. On the other hand, these nanoscale conjugated molecules possess several important properties that traditional inorganic semiconductors lack. For example, they are easily deposited on any low-cost substrates[3−7] such as glass, plastic, or metal foils. Therefore, OLED materials are particularly well suited for large-area displays.[4] Fabrication of high-resolution, full-color, and flat-panel displays[3] depends upon many factors. Apart from the optimization of device structure for OLEDs, A crucial step to improve the device performance is to design and synthesize new materials with improved properties[8−13] in charge conductivity, electroluminescence efficiency and power efficiency, thermal stability, operational lifetime, brightness, and color purity.

Jenekhe and collaborators[1] have synthesized a series of four n-type (electron transport) blue-light-emitting oligomers, oligoquinolines. They found that these organic materials can be used to fabricate high-efficiency light-emitting diodes. Recently, we have performed a theoretical investigation[14] of the optical absorption spectra of these molecules and utilized the natural transition orbitals to analyze the delocalization properties of several selected excited states, including the lowest one. The theoretical study has provided a detailed understanding of experimental measurements.

* To whom correspondence should be addressed. E-mail: jtao@lanl.gov.

† Theoretical Division and Center for Nonlinear Studies.

‡ Center for Integrated Nanotechnology.

10.1021/ct800523j CCC: $40.75
Published on Web 03/25/2009

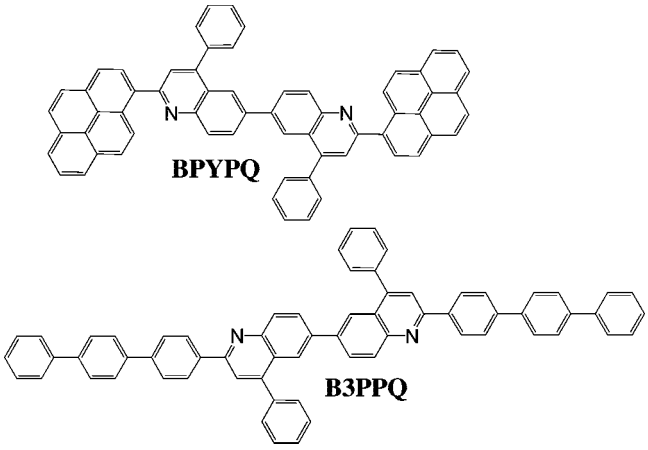

Figure 1. Molecular structures of the computationally studied blue-light-emitting oligoquinolines.

More recently, two new family members of the blue-light emitting oligoquinolines bearing pyrenyl and triphenyl end-groups have been synthesized and their important photochemistry properties such as optical absorption and emission as well as ionization potentials and electron affinities have been experimentally evaluated.[2] It has been found that these new pyrenyl- and triphenyl-bearing oligoquinoline molecules, 6,6′-bis(2-(1-pyrenyl)-4-phenylquinoline) (BPYPQ) and 6,6′-bis(2-(1-triphenyl)-4-phenylquinoline) (B3PPQ), have many desirable properties such as excellent thermal stability, high melt transitions, high quantum yields, and bright blue electroluminescence with high efficiency. They are highly emissive electron transport materials for OLEDs and have been used as emitters in recent fabrication of OLED devices. To get a better understanding of these experiments and to provide a deep physical insight into these phenomena, it is necessary to perform theoretical calculations. The method we choose for the calculation of dynamical properties such as optical absorption is time-dependent density functional theory,[15,16] while the ground-state density functional theory (DFT)[17] is employed to evaluate the equilibrium properties. TDDFT and DFT techniques currently provide optimal combination of accuracy and low computational cost for a broad variety of large molecules.

Kohn−Sham ground-state DFT[18,19] is the most popular method in electronic structure calculations because of its high computational efficiency. In this theory, only the exchange-correlation (XC) energy, which includes all unknown many-body effects, must be approximated as a functional of the electron density. In this paper, we employ several commonly used XC energy functionals to calculate the ionization potentials and the electron affinities of BPYPQ and B3PPQ molecules, whose chemical structures are shown in Figure 1. The density functionals we use here include two pure density functionals [the local spin density approximation (LSDA) and the Tao-Perdew-Staroverov-Scuseria (TPSS)[20] meta-generalized gradient approximation (meta-GGA)] and three hybrid functionals (TPSSh,[21] B3LYP,[22] and PBE0;[23,24] see discussion below). Then we employ the time-dependent DFT linear response theory[25,26] to calculate the optical absorptions of these two new family members of oligoquinolines, BPYPQ and B3PPQ. The dynamical XC potential is constructed, as usual, within the adiabatic approximation.[27] See refs 28−31 for the discussion of the nonadiabatic approximation.

Previous calculations[14,32−42] show that the adiabatic XC potentials constructed from a ladder of widely used density functionals yield excitation energies of molecules in fairly good agreement with experiments. Hybrid functionals such as PBE0 (a hybrid of PBE with 25% exact exchange) and TPSSh (a hybrid of TPSS with 10% exact exchange) yield excitation energies consistently in better agreement[14,42] with experiments than their parental nonhybrid functionals PBE GGA[43] and TPSS meta-GGA. In particular, PBE0, which benefits from the more amount of exact exchange, gives a very good performance in the prediction of low-lying excitations. This excellent improvement probably is a balanced effect between the error concellation between semilocal exchange and semilocal correlation (no exact exchange should be mixed in) and the improvement of the asymptotic behavior of the exchange potential (as much as exact exchange should be mixed in). Recently, Perdew, Staroverov, Tao, and Scuseria[44] have constructed a fourth-rung hyper-GGA, a fully nonlocal functional of the density, which satisfies many additional constraints beyond those[45,46] that the TPSS meta-GGA already satisfies. Specifically, we employ the TDDFT adiabatic PBE0 functional to evaluate the optical absorptions of BPYPQ and B3PPQ. The results obtained with the adiabatic LSDA, TPSS meta-GGA and hybrid TPSSh, and three-parameter hybrid B3LYP (with 1/5 exact exchange), are also presented for comparison. To spell out our results, a natural transition orbital analysis[47] for three selected excited states with the largest oscillator strengths is carried out.

II. Computational Method

All calculations are performed using the GAUSSIAN 03 program.[48] First we optimize the ground-state geometries of BPYPQ and B3PPQ by performing the self-consistent ground-state calculations with respective density functionals. Then we evaluate the vertical excitation energies of these two oligomers based on the optimized ground-state geometries with the respective adiabatic density functionals. Ionization potentials and electron affinities are estimated from the ground-state DFT self-consistent calculations. For consistency, the same basis set 6−31G(d) was used in all calculations. Because the Perdew−Wang parametrization[49] for the LSDA correlation energy is used as the local part in the PBE and TPSS correlation functionals, for consistency, this parametrization was used for all LSDA calculations. The TDDFT calculations of BPYPQ and B3PPQ in chloroform solvent were performed using PCM (polarizable continuum model)[50] method, which was shown[14] to yield almost the same results as CPCM (conductor-like PCM) method[51−53] for the family of oligoquinoline molecules. For systems with high dielectric constant, both methods are equivalent. See refs 54−57 for detailed discussion of PCM method.

III. Results and Discussion

A. Ionization Potentials and Electron Affinities. Ionization potentials are calculated as the difference in total

Table 1. Ionization Potentials (IPs) and Electron Affinities (EAs) (In Units of eV) of BPYPQ and B3PPQ, Evaluated with the Basis Set 6-31G(d) and Geometries Optimized on the Respective Density Functionals

		exptl	LSDA	TPSS	TPSSh	B3LYP	PBE0
BPYPQ	IP	5.86	5.91	5.65	5.82	5.93	6.11
	EA	2.66	2.00	1.75	1.66	1.54	1.59
	η[a]	1.60	1.96	1.95	2.08	2.20	2.26
B3PPQ	IP	5.78	6.01	5.70	5.90	6.03	6.24
	EA	2.58	1.96	1.70	1.59	1.46	1.51
	η[a]	1.60	2.03	2.00	2.16	2.29	2.37

[a] η is the molecular hardness defined by η =(IP − EA)/2.

Table 2. Singlet and Triplet Vertical Excitation Energies (ω_S^g, ω_T^q, n = the nth excited state) in eV, the Transition Oscillator Strength ($f^{abs,n}$), and the Dipole Moment of the Ground State in Debye of BPYPQ Molecule in Gas Phase (μ_g) and Chloroform Solution (μ_{sol}), Calculated Using the Five Adiabatic Density Functionals with the Basis Set 6−31G(d) and the Geometry Optimized on the Respective Density Functionals with the Same Basis (1 eV = 8065.5 cm^{-1} = 0.03675 hartree)[a]

	gas	gas	gas	gas	gas	gas	gas	bgas	sol	sol	sol	sol	sol	sol	sol	sol
	$\omega_S^{abs,1}$	$f^{abs,1}$	$\omega_S^{abs,4}$	$f^{abs,4}$	$\omega_S^{abs,14}$	$f^{abs,14}$	ω_T^{abs}	μ_g	$\omega_S^{abs,1}$	$f^{abs,1}$	$\omega_S^{abs,4}$	$f^{abs,4}$	$\omega_S^{abs,12}$	$f^{abs,12}$	ω_T^{abs}	μ_{sol}
LSDA	2.10	0.558	2.48	0.358	3.06	0.286	1.90	1.031	2.08	0.714	2.47	0.499	3.03	0.384	1.90	1.645
			$\omega_S^{abs,3}$	$f^{abs,3}$	$\omega_S^{abs,12}$	$f^{abs,12}$				$\omega_S^{abs,5}$	$f^{abs,5}$	$\omega_S^{abs,12}$	$f^{abs,12}$			
TPSS	2.21	0.473	2.58	0.392	3.17	0.334	1.85	1.112	2.19	0.610	2.56	0.536	3.15	0.400	1.86	1.761
			$\omega_S^{abs,5}$	$f^{abs,5}$	$\omega_S^{abs,11}$	$f^{abs,11}$				$\omega_S^{abs,5}$	$f^{abs,5}$	$\omega_S^{abs,10}$	$f^{abs,10}$			
TPSSh	2.61	0.852	3.16	0.506	3.48	0.271	1.88	1.138	2.58	1.081	3.14	0.503	3.45	0.314	1.89	1.784
			$\omega_S^{abs,5}$	$f^{abs,5}$	$\omega_S^{abs,9}$	$f^{abs,9}$					$\omega_S^{abs,5}$	$f^{abs,5}$	$\omega_S^{abs,7}$	$f^{abs,7}$		
B3LYP	2.89	1.275	3.44	0.501	3.64	0.092	1.98	1.122	2.85	1.998	3.42	0.513	3.61	0.122	1.98	1.744
			$\omega_S^{abs,5}$	$f^{abs,5}$	$\omega_S^{abs,9}$	$f^{abs,9}$					$\omega_S^{abs,5}$	$f^{abs,5}$	$\omega_S^{abs,14}$	$f^{abs,14}$		
PBE0	3.04	1.516	3.62	0.448	3.79	0.071	1.88	1.190	3.00	1.817	3.60	0.479	4.09	0.096	1.89	1.839
									ω_{1st}^{abs}		ω_{2nd}^{abs}		ω_{3rd}^{abs}			
exptl									3.26		3.60		4.34			

[a] Experimental values measured in chloroform are obtained from ref 2.

Table 3. Singlet and Triplet Vertical Excitation Energies (ω_S^g, ω_T^q, n = the nth excited state) in eV, the Transition Oscillator Strength ($f^{abs,n}$), and the Dipole Moment of the Ground State in Debye of B3PPQ Molecule in Gas Phase (μ_g) and Chloroform Solution (μ_{sol}), Calculated Using the Five Adiabatic Density Functionals with the Basis Set 6−31G(d) and the Geometry Optimized on the Respective Density Functionals with the Same Basis (1 eV = 8065.5 cm^{-1} = 0.03675 hartree)[a]

	gas	gas	gas	gas	gas	gas	gas	gas	sol	sol	sol	sol	sol	sol	sol	sol
	$\omega_S^{abs,1}$	$f^{abs,1}$	$\omega_S^{abs,4}$	$f^{abs,5}$	$\omega_S^{abs,13}$	$f^{abs,13}$	ω_T^{abs}	μ_g	$\omega_S^{abs,1}$	$f^{abs,1}$	$\omega_S^{abs,5}$	$f^{abs,5}$	$\omega_S^{abs,13}$	$f^{abs,13}$	ω_T^{abs}	μ_{sol}
LSDA	2.34	1.235	2.78	0.598	3.27	0.575	2.09	1.137	2.31	1.421	2.75	0.721	3.26	0.593	2.09	1.457
			$\omega_S^{abs,4}$	$f^{abs,4}$	$\omega_S^{abs,13}$	$f^{abs,13}$				$\omega_S^{abs,4}$	$f^{abs,4}$	$\omega_S^{abs,14}$	$f^{abs,14}$			
TPSS	2.49	1.209	2.93	0.425	3.42	0.503	2.079	1.234	2.46	1.378	2.89	0.430	3.42	0.391	2.09	1.602
			$\omega_S^{abs,5}$	$f^{abs,5}$	$\omega_S^{abs,16}$	$f^{abs,16}$				$\omega_S^{abs,10}$	$f^{abs,10}$	$\omega_S^{abs,15}$	$f^{abs,15}$			
TPSSh	2.86	1.779	3.42	0.502	3.95	1.047	2.16	1.267	2.83	1.998	3.74	0.772	3.92	0.856	2.18	1.636
			$\omega_S^{abs,7}$	$f^{abs,7}$	$\omega_S^{abs,12}$	$f^{abs,12}$				$\omega_S^{abs,6}$	$f^{abs,6}$	$\omega_S^{abs,11}$	$f^{abs,11}$			
B3LYP	3.12	2.197	3.86	0.542	4.09	0.923	2.29	1.265	3.08	2.429	3.81	0.498	4.06	0.642	2.30	1.632
			$\omega_S^{abs,6}$	$f^{abs,6}$	$\omega_S^{abs,12}$	$f^{abs,12}$				$\omega_S^{abs,6}$	$f^{abs,6}$	$\omega_S^{abs,12}$	$f^{abs,12}$			
BPE0	3.27	2.373	4.02	0.957	4.30	0.962	2.23	1.306	3.23	2.609	4.02	0.842	4.28	1.099	2.24	1.676
									ω_{1st}^{abs}		ω_{2nd}^{abs}					
exptl									3.32		4.04					

[a] Experimental values measured in chloroform are obtained from ref 2.

energies between the positive ion and the corresponding neutral in their ground states (using the spin-unrestricted DFT formalism) at their geometries optimized with respective density functionals. The results are displayed in Table 1, and the experimental estimates are also listed for comparison. From Table 1, we observe that LSDA, TPSS, and TPSSh give the IPs of BPYPQ and B3PPQ that are closest to the experimental estimates, while B3LYP and PBE0 yield slightly higher values, compared to the experimantal ones.

Electron affinities are calculated as the difference between the total energies of the negative ion and the corresponding neutral in their ground states (using the spin-unrestricted DFT formalism) at their geometries optimized with respective density functionals. The results are summarized in Table 1. We observe from Table 1 that all the density functional values are too low. The nonhybrid functionals (LSDA and TPSS meta-GGA) yield the estimates that are closer to the experimental values than hybrid functionals (TPSSh, B3LYP, and PBE0). As discussed in refs 21 and 58, since negative ions are unstable in the ground-state of semilocal local density functionals that suffer from self-interaction error, the ground-state energies of negative ions are estimated in practice with the artificial stabilization by the use of finite basis sets. That explains the large deviation of the density functional estimates of the electron affinities from the experimental values.

B. Optical Absorption. Tables 2 and 3 show the summary of the calculated properties of BPYPQ and B3PPQ in

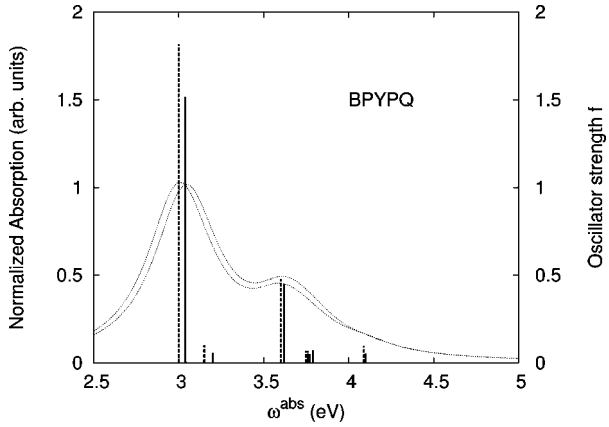

Figure 2. Normalized absorption *I* of eq 1 (in arbitrary units) (right side) and oscillator strength *f* (left side) of BPYPQ. The solid and dashed curves represent the normalized absorption in gas phase and solution, while the solid and dashed "sticks" represent the oscillator strength in gas phase and solution, respectively.

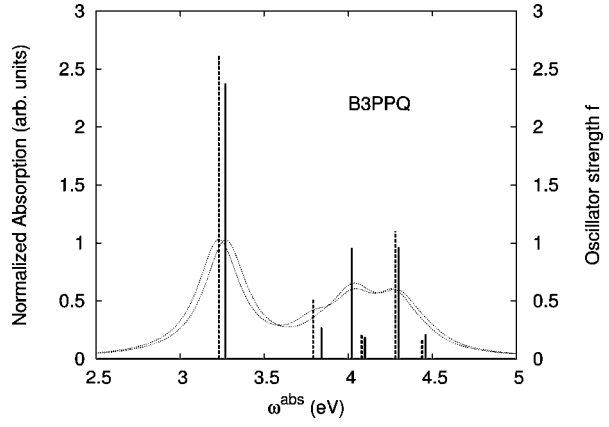

Figure 3. Normalized absorption *I* of eq 1 (in arbitrary units) (right side) and oscillator strength *f* (left side) of B3PPQ. The solid and dashed curves represent the normalized absorption in gas phase and solution, while the solid and dashed "sticks" represent the oscillator strength in gas phase and solution, respectively.

gas phase and in solution, respectively. These calculated properties include the excitation energies of three singlet states with the largest oscillator strengths in the UV−vis region, the corresponding oscillator strengths, and the excitation energy of the first triplet state, in gas phase and solution. The ground-state dipole moments of BPYPQ and B3PPQ in gas phase and solution are also calculated and presented in Tables 2 and 3, respectively. The experimentally observed excitation energies are listed for comparison. Of course, this comparison can be made only approximately because vibrational progression and disorder effects are not included in our calculations. This can make a difference of up to 0.1−0.2 eV.

From Table 2, we observe that the first or lowest-frequency peak of BPYPQ occurs at 3.00 eV (the experimental value is 3.26 eV) with the largest oscillator strength $f = 1.82$ and that a higher-frequency peak occurs at 3.60 eV (the same as the experimental value) with the oscillator strength $f = 0.48$, almost three times smaller than the largest oscillator strength. The third or the highest-frequency absorption peak occurs at about 4.09 eV (4.34 eV for the experimental measurement), with a very small oscillator strength $f = 0.1$. The oscillator strength of the third absorption peak is underestimated significantly with the adiabatic B3LYP and PBE0 functionals. The adiabatic LSDA, TPSS, and TPSSh functionals yield a more realistic oscillator strength, although it is still too small, compared to the experimental observation, where the experimental intensity of the third absorption band is quite noticeable.[2] This discrepancy of theory from experiment for the third peak absorbance may arise from many effects such as temperature, disorder, vibrational progression, etc. These factors have not been taken into consideration in our calculations. We also observe a persistent red shift for the first two peaks from gas phase to solution. This red shift (of about 10 meV) also occurs for the lowest triplet excitation. The dipole moment of BPYPQ is vanishingly small if all the atoms are in a same plane because of its high symmetry. However, this geometry is not the ground-state geometry. In the ground state, there are dihedral angles between two benzene rings connected by a σ-bond. These dihedral angles effectively reduce the symmetry of the molecule, resulting in a large ground-state dipole moment. While the effect of the solvent−solute interaction on the optical absorption is small, it has a significan effect on the ground-state dipole moment and causes the noticeable increase of the oscillator strength in solution, compared to that in gas phase. The absorptions calculated with other adiabatic TDDFT functionals are in fairly good agreement with experiments. The accuracy increases when we go from LSDA, TPSS meta-GGA, TPSSh, and B3LYP to PBE0.

Table 3 shows that in gas phase the first two absorptions of B3PPQ occur at 3.27 and 4.02 eV, respectively, with the oscillator strength of the first peak being about twice that of the second peak. Interestingly, our calculation shows that there should be another absorption peak, which occurs at a higher frequency 4.30 eV. The absorption intensity of the third peak is nearly the same as the second. Since these two peaks are located closely, they may combine to form a broader single peak. Therefore, we may only observe two absorption peaks in total in the experiment. In solution, the three peaks are expected to occur at slightly lower frequency because of the red shift, as shown in Table 3. The solvent−solute effects on the absorption and the ground-state moment are the same as those for BPYPQ.

To simulate the experimentally observed absorptions with our calculated data (see Figures 2 and 3), a simple analytic expression[14] for the normalized absorption intensity or peak magnitude is assumed as

$$I(\omega) = \sum_i f(\omega_i)\delta_m(\omega - \omega_i) \Big/ \sum_i f(\omega_i) \qquad (1)$$

where $\delta_m(x)$ is a δ-like function defined by

$$\delta_m(x) = \frac{m}{\pi}\frac{1}{1 + m^2x^2} \qquad (2)$$

Here m is determined by a fit to experiments; $m = 5.0$ for BPYPQ and 7.0 for B3PPQ. This form has been used[14] to

Table 4. TDDFT Natural Transition Orbital Analysis for the Three Excited States with the Largest Oscillator Strengths in BPYPQ in Gas Phase[a]

Excited state	Electron	Hole
$\|1\rangle$ $\Delta E = 3.04$ eV $f = 1.516$ $W = 92.4\%$	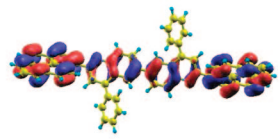	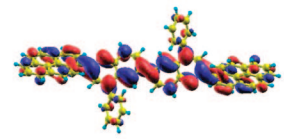
$\|5\rangle$ $\Delta E = 3.62$ eV f = 0.448 $W = 60.4\%$	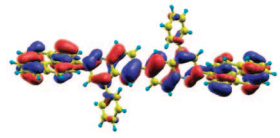	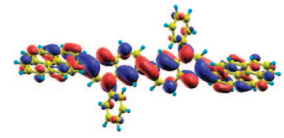
$\|9\rangle$ $\Delta E = 3.79$ eV f = 0.071 $W = 58.1\%$	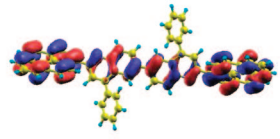	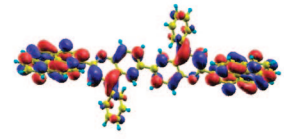

[a] ΔE is the excitation energy, f is the corresponding oscillator strength, and W is the weight of the plotted orbital in the respective transition density matrix.

Table 5. TDDFT Natural Transition Orbital Analysis for the Three Excited States with the Largest Oscillator Strengths in B3PPQ in Gas Phase[a]

Excited state	Electron	Hole
$\|1\rangle$ $\Delta E = 3.27$ eV $f = 2.373$ $W = 94.9\%$	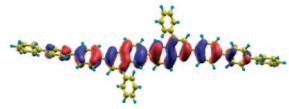	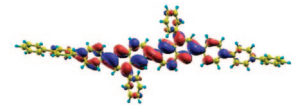
$\|6\rangle$ $\Delta E = 4.02$ eV f = 0.957 $W = 57.6\%$	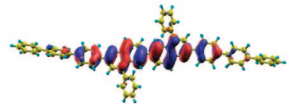	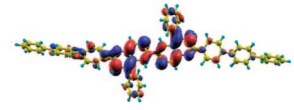
$\|12\rangle$ $\Delta E = 4.30$ eV f = 0.962 $W = 52.6\%$	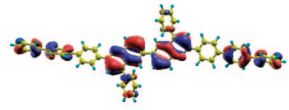	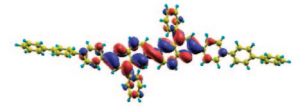

[a] ΔE is the excitation energy, f is the corresponding oscillator strength, and W is the weight of the plotted orbital in the respective transition density matrix.

simulate the optical absorption spectra of other four family members of oligoquinoline molecules. In our simulation, we did not employ the most commonly used Gaussian function. These two functions[59] (eq 1 and Gaussian function) have similar properties and are equivalent in the limit of $m \rightarrow \infty$, but the former gives a better fit to experiments. As displayed in Figure 2, our simulation for the absorption of BPYPQ shows two peaks, whose locations or absorption frequencies are close to the experimentally observed, while the third peak is almost invisible because of a very small absorption intensity. Figure 3 shows a large absorption peak at the lowest frequency and other two smaller peaks at higher frequencies, latter of which may combine to form a broader one.

Finally, we employ the natural transition orbital representation for excited states to analyze the corresponding excited states. The results are plotted and displayed in Tables 4 and 5, respectively. The orbitals we employ here are calculated

with the adiabatic PBE0 functional, which yield the most accurate excitation energies for the entire family of oligoquinoline molecules. It is clear that these low-lying excited states arise from $\pi-\pi^*$ excitations, as illustrated by their transition orbitals shown in Tables 4 and 5. From the weight ($W = 92\%$), we can see that the lowest excited state, $|1\rangle$, can be well represented by a single-pair of transition orbitals (see Table 4). It arises from a delocalized excitation involving the entire conjugated backbone of the BPYPQ oligomer. The side phenyl rings do not participate substantially in this optical excitation. Excited state $|5\rangle$ contributing to the second absorption peak is largely delocalized in the middle section of the molecule, compared to excited state $|1\rangle$, while excited state $|9\rangle$ contributing to the third absorption peak is mainly delocalized in the endgroups of the molecule. We note that excited states $|5\rangle$ and $|9\rangle$ are multiconfigurational, that is, they can be represented only by several pairs of transition orbitals. Here only the dominant ones are shown in Table 4.

The B3PPQ orbitals are slightly less delocalized, compared to those of BPYPQ, while the molecular structure of the former has a longer backbone. This is reflected by the higher excitation energies of B3PPQ. The same trend for the lowest triplet excitation is also observed by comparing Table 2 with Table 3. The oscillator strengths of B3PPQ corresponding to three selected excitations are much larger than those of BPYPQ. From Table 5, we can see that, like BPYPQ, these selected excited states also arise from $\pi-\pi^*$ excitations. The large weight $W = 95\%$ of the lowest excited-state suggests that excited state $|1\rangle$ can essentially be represented by a single-pair of transition orbitals. The side- and end-phenyl rings do not participate in this lowest-frequency optical excitation. Excited state $|6\rangle$ responsible for the second absorption peak is mainly delocalized in the middle section of the molecule, while excited state $|12\rangle$ is partly delocalized in the middle section and partly in the ending sections. Compared to excited states $|1\rangle$ and $|6\rangle$, it is much more delocalized. Table 5 also shows that there are slight charge redistributions during the excitations, with the electronic density flow toward the center of the molecules.

IV. Conclusion

In this paper, we have employed the adiabatic TDDFT approach to study the optical absorption of two new family members of the blue-light emitting oligoquinolines bearing pyrenyl and triphenyl endgroups, BPYPQ and B3PPQ, in gas phase and chloroform ($CHCl_3$) solution. Ionization potentials and electron affinities, which are important in photochemistry, are also calculated using the ground-state DFT. Our calculations of excitation energies are in good agreement with the experimental measurements in chloroform solution, while the absorption intensity or oscillator strength for two higher-frequency absorptions are significantly underestimated for BPYPQ. The ionization potentials agree well with the experimental estimates, while the electron affinities are underestimated.

Our results show that there are two absorption peaks for B3PPQ molecules in gas phase and solution, and the second peak located at a higher frequency may be split into two peaks, as experimentally observed for BPYPQ molecule. The first absorption peak arises from the lowest singlet−singlet transition, whereas the other arises from the multiconfigurational transition. Our simulation of the experimental spectra with the TDDFT data calculated from the adiabatic PBE0 functional shows that there are two main absorption peaks. This prediction agrees with experiments. However, it is questionable whether the third peak can be observed. This discrepancy of the theory from the experimental observation for the third peak intensity may arise from the fact that many effects (temperature, disorder, etc.) that affect the experiment have not been taken into account in our calculations. Our calculations also show that the solvent effects on computed electronic transitions are negligible. To get a detailed understanding of these excitations, an analysis of the natural transition orbitals corresponding to the selected excited states has been made. We find that for both BPYPQ and B3PPQ molecules, the low-lying optically active excited states are $\pi-\pi^*$ excitations with varying degree of spatial delocalization and charge transfer character.

We emphasize here that the order of accuracy of the five adiabatic density functionals in predicting the low-lying excitation energies of molecules, as found in our previous studies,[14,42] that is, LSDA < TPSS < TPSSh < B*3*LYP < PBE0, continue to hold, as shown in Tables 2 and 3.

Acknowledgment. The authors thank Ekaterina Badaeva for technical help and Chao Wu for helpful discussions. This work was supported by the U.S. Department of Energy under the Grant No. LDRD-PRD X9KU at Los Alamos National Laboratory.

References

(1) Tonzola, C. J.; Kulkarni, A. P.; Gifford, A. P.; Kaminsky, W.; Jenekhe, S. A. *Adv. Funct. Mater.* **2007**, *17*, 863.

(2) Hancock, J. M.; Gifford, A. P.; Tonzola, C. J.; Jenekhe, S. A. *J. Phys. Chem. C* **2007**, *111*, 6875.

(3) Forrest, S. R. *Nature* **2004**, *428*, 911.

(4) Kraft, A.; Grimsdale, A. C.; Holmes, A. B. *Angew. Chem., Int. Ed.* **1998**, *37*, 402.

(5) Mitschke, U.; Bauerle, P. J. *J. Mater. Chem.* **2000**, *10*, 1471.

(6) Kim, D. Y.; Cho, H. N.; Kim, C. Y. *Prog. Polym. Sci.* **2000**, *25*, 1089.

(7) Kulkarni, A. P.; Tonzola, C. J.; Babel, A.; Jenekhe, S. A. *Chem. Mater.* **2004**, *16*, 4556.

(8) Heeger, A. J.; Heeger, D. J.; Langan, J.; Yang, Y. *Science* **1995**, *270*, 1642.

(9) Sirringhaus, H.; Kawase, T.; Friend, R. H.; Shimoda, T.; Inbasekaran, M.; Wu, W.; Woo, E. P. *Science* **2000**, *290*, 2123.

(10) Menard, E.; Meitl, M.; Sun, Y.; Park, J.-U.; Shir, D.-L.; Nam, Y.-S.; Jeon, S.; Rogers, J. *Chem. Rev.* **2007**, *107*, 1117.

(11) Granstrom, M.; Petritsch, K.; Arias, A. C.; Lux, A.; Andersson, M. R.; Friend, R. H. *Nature* **1998**, *395*, 257.

(12) Yu, G.; Gao, J.; Hummelen, J. C.; Wudl, F.; Heeger, A. J. *Science* **1995**, *270*, 1789.

(13) Sirringhaus, H.; Brown, P. J.; Friend, R. H.; et al. *Nature* **1999**, *401*, 685.

(14) Tao, J.; Tretiak, S.; Zhu, J.-X. *J. Phys. Chem. B* **2008**, *112*, 13701.

(15) Giuliani, G. F.; Vignale, G. *Quantum Theory of the Electron Liquid*; Cambridge University Press: 2005.

(16) *Time-Dependent Density Functional Theory*; Lecture Notes in Physics Vol. 706; Marques, M. A. L., Ullrich, C. A., Nogueira, F., Rubio, A., Burke, K., Gross, E. K. U., Eds.; Springer: Berlin, 2006.

(17) Perdew, J. P.; Kurth, S. In *A Primer in Density Functional Theory*; Lecture Notes in Physics Vol. 620; Fiolhais, C., Nogueira, F., Marques, M., Eds.; Springer: Berlin, 2003.

(18) Kohn, W.; Sham, L. J. *Phys. Rev.* **1965**, *140*, A1133.

(19) Parr, R. G.; Yang, W.; *Density Functional Theory of Atoms and Molecules*; Oxford University Press: Oxford, U.K., 1989.

(20) Tao, J.; Perdew, J. P.; Staroverov, V. N.; Scuseria, G. E. *Phys. Rev. Lett.* **2003**, *91*, 146401.

(21) Staroverov, V. N.; Scuseria, G. E.; Tao, J.; Perdew, J. P. *J. Chem. Phys.* **2003**, *119*, 12129; **2004**,, *121*, 11507(E).

(22) Stephens, P. J.; Devlin, F. J.; Chabalowski, C. F.; Frisch, M. J. *J. Phys. Chem.* **1994**, *98*, 11623.

(23) Ernzerhof, M.; Scuseria, G. E. *J. Chem. Phys.* **1999**, *110*, 5029.

(24) Adamo, C.; Barone, V. *J. Chem. Phys.* **1999**, *110*, 6158.

(25) Petersilka, M.; Gossmann, U. J.; Gross, E. K. U. *Phys. Rev. Lett.* **1996**, *76*, 1212.

(26) Bauernschmitt, R.; Ahlrichs, R. *Chem. Phys. Lett.* **1996**, *256*, 454.

(27) Zangwill, A.; Soven, P. *Phys. Rev. Lett.* **1980**, *45*, 204; *Phys. Rev. A* **1980**,, *21*, 1561.

(28) Gross, E. K. U.; Kohn, W. *Phys. Rev. Lett.* **1985**, *55*, 2850.

(29) Vignale, G.; Kohn, W. *Phys. Rev. Lett.* **1996**, *77*, 2037.

(30) Tao, J.; Vignale, G. *Phys. Rev. Lett.* **2006**, *97*, 036403.

(31) Tao, J.; Vignale, G.; Tokatly, I. V. *Phys. Rev. B* **2007**, *76*, 195126.

(32) Tozer, D. J.; Handy, N. C. *J. Chem. Phys.* **1998**, *109*, 10180.

(33) Stratmann, R. E.; Scuseria, G. E. *J. Chem. Phys.* **1998**, *109*, 8218.

(34) Adamo, C.; Scuseria, G. E.; Barone, V. *J. Chem. Phys.* **1999**, *111*, 2889.

(35) Schipper, P. R. T.; Gritsenko, O. V.; van Gisbergen, S. J. A.; Baerends, E. J. *J. Chem. Phys.* **2000**, *112*, 1344.

(36) Sala, F. D.; Görling, A. *Int. J. Quantum Chem.* **2003**, *91*, 131.

(37) Jacquemin, D.; Bouhy, M.; Perpete, E. A. *J. Chem. Phys.* **2006**, *124*, 204321.

(38) Tretiak, S. *Nano Lett.* **2007**, *7*, 2201.

(39) Adams, R. D.; Captain, B.; Hall, M. B.; Trufan, E.; Yang, X. Z. *J. Am. Chem. Soc.* **2007**, *129*, 12328.

(40) Sancho-García, J. C. *Chem. Phys. Lett.* **2007**, *439*, 236.

(41) Igumenshchev, K. I.; Tretiak, S.; Chernyak, V. Y. *J. Chem. Phys.* **2007**, *127*, 114902.

(42) Tao, J.; Tretiak, S.; Zhu, J.-X. *J. Chem. Phys.* **2008**, *128*, 084110.

(43) Perdew, J. P.; Burke, K.; Ernzerhof, M. *Phys. Rev. Lett.* **1996**, *77*, 3865.

(44) Perdew, J. P.; Staroverov, V. N.; Tao, J.; Scuseria, G. E. *Phys. Rev. A* **2008**, *78*, 052513.

(45) Staroverov, V. N.; Scuseria, G. E.; Tao, J.; Perdew, J. P. *Phys. Rev. B* **2004**, *69*, 075102.

(46) Perdew, J. P.; Ruzsinszky, A.; Tao, J.; Staroverov, V. N.; Scuseria, G. E.; Csonka, G. I. *J. Chem. Phys.* **2005**, *123*, 062201.

(47) Martin, R. L. *J. Chem. Phys.* **2003**, *118*, 4775.

(48) Frisch, M. J., Trucks, G. W.; Schlegel, H. B.; Scuseria, G. E.; Robb, M. A.; Cheeseman, J. R.; Zakrzewski, V. G.; Montgomery, Jr., J. A.; Stratmann, R. E.; Burant, J. C.; Dapprich, S.; Millam, J. M.; Daniels, A. D.; Kudin, K. N.; Strain, M. C.; Farkas, O.; Tomasi, J.; Barone, V.; Cossi, M.; Cammi, R.; Mennucci, B.; Pomelli, C.; Adamo, C.; Clifford, S.; Ochterski, J.; Petersson, G. A.; Ayala, P. Y.; Cui, Q.; Morokuma, K.; Malick, D. K.; Rabuck, A. D.; Raghavachari, K.; Foresman, J. B.; Cioslowski, J.; Ortiz, J. V.; Stafanov, B. B.; Liu, G.; Liashenko, A.; Piskorz, P.; Komaromi, I.; Gomperts, R.; Martin, R. L.; Fox, D. J.; Keith, T.; Al-Laham, M. A.; Peng, C. Y.; Nanayakkara, A.; Gonzalez, C.; Challacombe, M.; Gill, P. M. W.; Johnson, B.; Chen, W.; Wong, M. W.; Andres, J. L.; Gonzalez, C.; Head-Gordon, M.; Replogle, E. S.; Pople, J. A. *Gaussian 03.*; Gaussian, Inc.: Pittsburgh PA, 2003.

(49) Perdew, J. P.; Wang, Y. *Phys. Rev. B* **1992**, *45*, 13244.

(50) Cancès, E.; Mennucci, B.; Tomasi, J. *J. Chem. Phys.* **1997**, *107*, 3032.

(51) Barone, V.; Cossi, M. *J. Phys. Chem. A* **1998**, *102*, 1995.

(52) Cossi, M. *Chem. Phys. Lett.* **2003**, *384*, 179.

(53) Cossi, M.; Rega, N.; Scalmani, G.; Barone, V. J. *Comp. Chem.* **2003**, *24*, 669.

(54) Cancès, M. T.; Mennucci, B.; Tomasi, J. *J. Chem. Phys.* **1997**, *107*, 3032.

(55) Cossi, M.; Barone, V.; Mennucci, B.; Tomasi, J. *Chem. Phys. Lett.* **1998**, *286*, 253.

(56) Mennucci, B.; Tomasi, J. *J. Chem. Phys.* **1997**, *106*, 5151.

(57) Mennucci, B.; Cancès, E.; Tomasi, J. *J. Phys. Chem. B* **1997**, *101*, 10506.

(58) Rösch, N.; Trickey, S. B. *J. Chem. Phys.* **1997**, *106*, 9840.

(59) Arfken, G. *Mathematical Methods for Physicists*, 3rd ed.; Academic Press: New York, 1985.

CT800523J